Inverse potential scattering in duct acoustics

Barbara J. Forbes[a)]
Phonological Ltd., P.O. Box 43925, London NW2 1DJ, United Kingdom

E. Roy Pike
Department of Physics, King's College London, Strand, London, WC2R 2LS, United Kingdom

David B. Sharp
Department of Environmental and Mechanical Engineering, The Open University, Walton Hall, Milton Keynes, MK7 6AA, United Kingdom

Tuncay Aktosun
Department of Mathematics and Statistics, Mississippi State University, Mississippi State, Mississippi 3976

(Received 14 June 2005; accepted 24 October 2005)

The inverse problem of the noninvasive measurement of the shape of an acoustical duct in which one-dimensional wave propagation can be assumed is examined within the theoretical framework of the governing Klein–Gordon equation. Previous deterministic methods developed over the last 40 years have all required direct measurement of the reflectance or input impedance but now, by application of the methods of inverse quantum scattering to the acoustical system, it is shown that the reflectance can be algorithmically derived from the radiated wave. The potential and area functions of the duct can subsequently be reconstructed. The results are discussed with particular reference to acoustic pulse reflectometry. © *2006 Acoustical Society of America.* [DOI: 10.1121/1.2139618]

PACS number(s): 43.20.Mv, 43.20.Ye, 43.58.Gn, 43.60.Pt [SFW] Pages: 65–73

I. INTRODUCTION

The noninvasive measurement of the internal geometry of an acoustical duct is a problem that has long interested researchers in all of mechanical engineering, medical diagnostics, musical acoustics, and speech analysis (see Refs. 1 and 2 for a review). Although it has been established for some 40 years that the transfer function of such a duct does not uniquely determine its area function,[2] even in the lossless case, it is also well known that the area function is completely specified by the input impedance or, equivalently, the reflectance.[3–8] In recent years, accurate and fast duct reconstructions have been obtained by the acoustic pulse reflectometry (APR) method[9–16] which, since the experimental apparatus is relatively portable, has also proved ideally suited to field measurements. Despite this efficiacy, the APR methodology demands that the temporal reflectance be measured directly, and so the experimental protocol requires up to 12 m of extraneous control tubing for the elimination of secondary reflections from the source boundary. Further, all measurements must be taken in the same place and so the method cannot be used to probe the shape of the vocal tract during normal phonation at the glottis. Indeed, due to the nonuniqueness, it is known that the vocal-tract area function cannot be deterministically reconstructed from the radiated speech wave alone, although statistical methods have been attempted.[17–21] Nevertheless, recent results from the mathematical literature report existence proofs for the temporal inversion of the Webster equation from radiated data and known initial conditions.[22–24]

In this paper, a novel and computationally efficient, frequency-domain method for the deterministic acoustical duct inversion is presented, which makes no demands on the direct measurement of either reflectance or impedance. Rather, the reflectance is mathematically derived from the wave radiated in response to a high-impedance source. Since the algorithms naturally incorporate any number of reflections between the source and radiating end, which may be any distance apart, the results are of relevance both in acoustic pulse reflectometry and to the speech inverse problem in particular.

Section II reviews standard inversion methods that reconstruct the area function of an acoustical duct from measurements of the reflected wave. Section III presents an alternative methodology that allows the wave-mechanical reflectance to be derived from the resonance spectrum of the radiated wave, yielding the "potential" function of the duct. The relationship between the potential and area functions is discussed. Section IV validates the proposed inversion methodology through numerical simulations at varying bandwidth. Section V discusses further issues that become relevant in experimental contexts.

II. BACKGROUND

Figure 1 gives a schematic diagram of an acoustic pulse reflectometer,[1,10] typically used for the noninvasive measurement of narrow bore acoustical ducts. An electrical pulse

[a)]Also at: Department of Physics, King's College London, Strand, London, WC2R 2LS, UK; electronic mail: forbes@phonologica.com

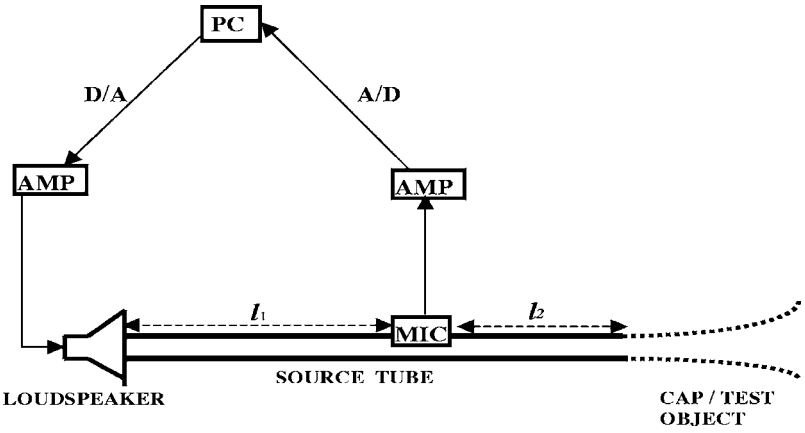

FIG. 1. A schematic diagram of the acoustic pulse reflectometer.

produced by D/A conversion of a digital array is amplified and the resultant pressure wave travels along a length of control tubing, the "source" tube. Reflections from the test object are recorded at the microphone, before A/D conversion and analysis. In the determination of the unknown input impulse response or filter function, $z(t)$, two consecutive measurements are necessary: a calibration measurement of the input pulse, the source function $x(t)$, obtained by sampling the signal reflected back from the rigid termination of the source tube capped with a removable end piece; and one of the reflections, $y(t)$, obtained when the cap is replaced by the test object. The control length l_1 gives the approximation of a source at infinity, allowing $y(t)$ to be cleanly sampled without interference from higher-order reflections at the boundary.[11] If reflections are to be measured for a time $T=50$ ms, for example, l_1 must be set to around 8.5 m. The length l_2, typically[13] set to 4 m, ensures that the incident pulse has completely passed the microphone before recording of the reflections begins.

The system is described by a Fredholm equation of the first kind, namely

$$y(t) = \int_0^t x(t-\tau)z(\tau)d\tau, \quad 0 \leqslant t \leqslant T, \tag{1}$$

from which $z(t)$ must be obtained by a deconvolution procedure before being submitted to a bore reconstruction algorithm.[1,25] It is known[6,26] that this deconvolution is ill posed in the context of finite experimental bandwidths, and previous work by the authors[1] has discussed both theoretical and experimental regularization procedures. However, it was shown by us that propagation losses[27] (−2dB/m at 1 kHz) within the long lengths of control tubing can reduce the effective range of the loudspeaker from the nominal limit of 18 kHz to around just 6 kHz. Since the axial resolution, Δ, in the bore reconstruction is defined by the effective signal bandwidth, f_{eff}, as

$$\Delta = \frac{c}{4f_{\text{eff}}}, \tag{2}$$

for c the speed of sound in free space, neglecting dissipation (taken to be 344 m s^{-1} at 20 °C), it was thus shown that the control tubing causes an increase in resolution from a nominal value of 3.9 mm (at 44.1 kHz sampling) to just 1.6 cm (around four sample points). Clearly, the APR apparatus could be substantially streamlined and the precision and accuracy of the duct reconstruction much improved if an alternative to the direct measurement of the reflections, $y(t)$, could be found.

Available bore reconstruction algorithms assume plane-wave propagation,[25,28] and previous work[1] has noted that the inverse mapping from reflectance (or impedance) to area function will only be fully regularized for algorithms that take into account higher mode solutions,[29–32] which may propagate at high bandwidth in wide and/or strongly expanding objects. To assess the relative contribution of propagation losses and experimental higher modes to the ill-posedness of the bore reconstruction problem, therefore, numerical simulations were made of a conical horn of length 7.5 cm and input and terminating radii $r_0=4.8$ mm and $r_l=3$ cm, respectively. A lead-in tube of 34.4 cm length was assumed for the control of pressure offsets[15] and an ideal closed termination ($Z_{\text{rad}} \to \infty$) was chosen to minimize the effect of the radiation impedance, elucidating multimodal phenomena due to changes in the bore.

The multimodal PAK[29,30] algorithms were implemented numerically at varying mode order, and "forward" solutions for the input impedance were obtained, yielding impulse responses, $z(t)$, that were implemented in a standard, plane-wave, inversion. Lossy forms of both the forward and inverse algorithms were adopted.[31,33] [Due to strongly evanescent higher order modes, convergence in the numerical solution of the PAK algorithms may require an extremely small cylindrical discretization, d, which should be smaller than the spatial sampling length. The reported simulations, for example, were run at $d=0.1$ mm (one-mode solution), and $d=0.02$ mm (four-mode solution), $\Delta=0.2$ mm, with numerical problems due to the inversion of singular matrices becoming evident at higher orders. For these parameters, a one-mode solution takes around 30 min to compute on a 1.8 GHz PC with 512 Mbytes RAM under MATLAB for Windows.] Results were obtained first at an idealized, high bandwidth of 400 kHz, corresponding to an axial resolution of 0.2 mm.

Figure 2(a) illustrates that, when plane-wave propagation is assumed in both the forward and inverse algorithms, the bore reconstruction agrees with the nominal bore radius to within a maximum numerical error of around 0.7% at the mouth. When the first higher mode is included in the forward

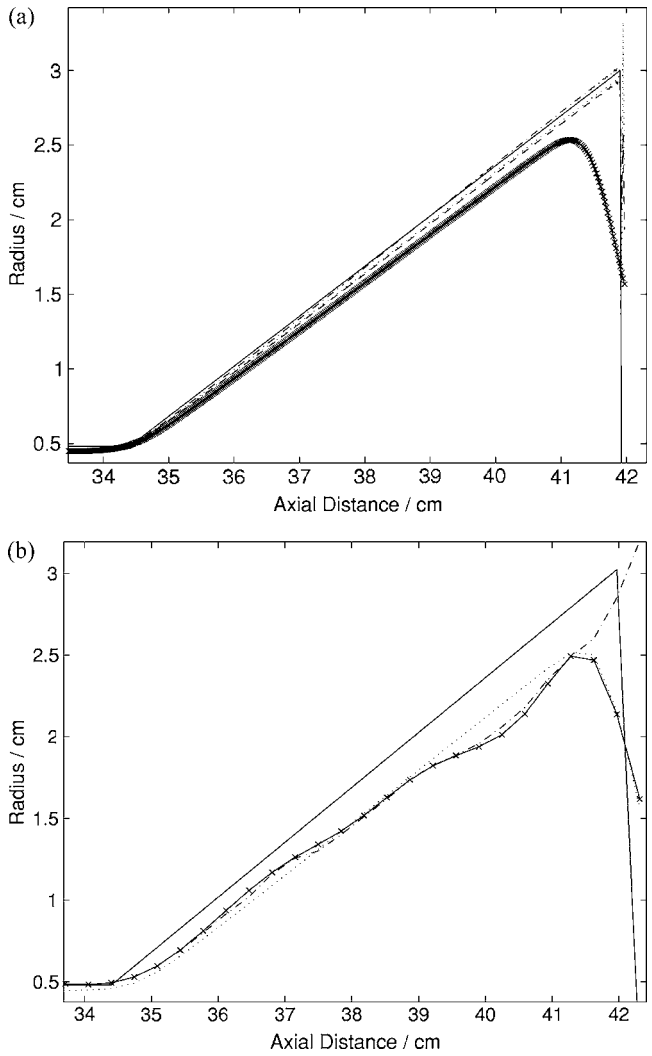

FIG. 2. (a) Conical duct inversion for multimodal impulse response: theoretical radius (—), one mode (---), two mode (···), three mode (---), one mode filtered at 6 kHz (×). (b) Conical duct inversion for multimodal impulse response: theoretical radius (—), one mode filtered at 6 kHz (···), experimental (×), experimental open-ended (---). Both reconstructions include a 34.4 cm lead-in tube.

simulation (cut-on 7 kHz), the error rises to some 1.7% due to the ill-posedness of the plane-wave reconstruction. Adding the second higher mode (cut-on 13 kHz) increases the error by around 1%, to 2.7%. However, this error remains stable with the addition of the next higher mode (cut-on 19 kHz). A far more dramatic effect is found by filtering the plane-wave solution at a half-power point of 6 kHz, below higher mode cut-on but representative of the reduced experimental bandwidth that results from propagation losses. Figure 2(a) now shows that the effective axial resolution falls to around 1.6 cm so that rapid changes in the bore profile take three to four nominal sample points to manifest, introducing an underestimation in the bore reconstruction that rises to as much as 30%.

Indeed, Fig. 2(b) shows that there is good agreement between the simulated, filtered, plane-wave solution and that found by experiment. [An experimental cone with a removable flat metal plate at the termination was machined to the dimensions of the simulations. The reconstruction for a closed end agreed with that for an open end, on removal of the plate, to better than 3%–4% within the main part of the bore.] Figure 2(b) also shows the experimental reconstruction of an open-ended cone, in which additional multimodal effects (*albeit* evanescent) can be assumed. Despite this, the closed and open-ended reconstructions are in close agreement in the main part of the cone.

These results therefore suggest that experimental errors arising from propagation losses may well outweigh those that would arise from higher mode solutions if high bandwidths could be attained. Thus, it can be concluded that methods for eliminating the need for control tubing in the APR apparatus are required.

III. REGULARIZED METHODOLOGY

Although methods for simplifying the APR apparatus have been proposed,[7,11,16] all are constrained by the requirement that the impulse response, $z(t)$, be estimated by direct measurement of the reflections, $y(t)$. It is now possible to present a method that allows $y(t)$ to be derived from noninvasive measurements of the radiated wave. Since multiple reflections are a natural part of the theoretical model, no control tubing is required in the experimental methodology so that propagation losses within the system are dramatically reduced. The concommitant increase in bandwidth substantially regularizes the deconvolution of Eq. (1) and, hence, the duct reconstruction problem.

A. Forward problem: The acoustical Klein–Gordon equation

The results of the previous section suggest that, for many applications in duct acoustics, a plane-wave approximation is effective. It can now be shown that a particularly elegant description exists within the theoretical framework of the governing Klein–Gordon equation.

It has previously been shown that the Webster equation, valid for one-dimensional compressible flow in the linear, adiabatic and nonviscous approximations, can be reduced to a Klein-Gordon equation,[34–38] namely

$$\frac{\partial^2\Psi(x,t)}{\partial t^2} = c^2\left\{\frac{\partial^2\Psi(x,t)}{\partial x^2} - U(x)\Psi(x,t)\right\}, \tag{3}$$

for a "wave function," $\Psi(x,t)$, such that for $p(x,t)$ the excess pressure and $S(x)$ the cross-sectional area of the wave front,

$$\Psi(x,t) = p(x,t)\sqrt{S(x)}. \tag{4}$$

The parameter $U(x)$ is defined as

$$U(x) = \frac{d^2\sqrt{S(x)}/dx^2}{\sqrt{S(x)}}, \tag{5}$$

and is mathematically analogous to the potential function of quantum mechanics. Where no confusion is likely to arise, such as in the present paper, it can thus be referred to as the "potential function." Otherwise, since it refers to a geometry rather than an energy, it should be referred to as the horn function.[34] A unique area function can be found from the

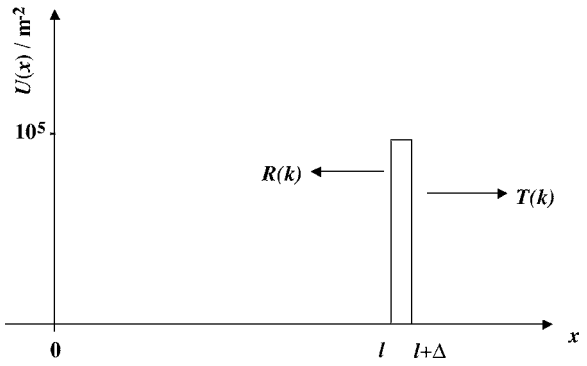

FIG. 3. Schematic potential-function profile of duct terminated in barrier equivalent to a radiation impedance, $U_0=10^5$ m^{-2}, $\Delta=1$ mm.

"potential" function by solution of the homogeneous equation

$$\frac{d^2\sqrt{S(x)}}{dx^2} - U(x)\sqrt{S(x)} = 0, \tag{6}$$

given two known initial conditions on the area.

Previous work[35,36] has considered piecewise constant potential functions, for which $U(x)=U_0$, and it has been shown that a wave-mechanical barrier of approximate height $U_0=1.0\times10^5$ m^{-2} and width $\Delta=1$ mm shares the major characteristics of standard impedance approximations, such as the infinite baffle. In fact, the square barrier corresponds to an infinite cone, whose initial radius and slope are continuous with those of the duct and in which the pressure amplitude falls off with $1/x$, as for a spherically outgoing wave. For analytic and numerical modeling purposes, therefore, the square barrier may be used as a one-dimensional equivalent to commonly adopted radiation impedances. The main advantage of this is that the singularity in the plane-wave potential function, as noted by Benade and Jansson,[34] can be approximated by finite parameters. Subsequently, both the wave function and its first derivative can be matched across the point of expansion into free space, yielding an analytic expression[35,36] for the radiated wave in which energy is fully conserved. This is in contrast to the Wertzel–Kramers–Brillouin approximation adopted by Benade and Jansson, which neglects backward traveling solutions within the lip region and is, in fact, known to be quite inappropriate for changes that occur on scales short in comparison to a wavelength.[39]

A barrier equivalent to the radiation impedance for a duct of length l is illustrated in Fig. 3, along with its transmitted, $T(k)$, and reflected, $R(k)$, waves, for k the free space wave number and $\omega=ck$. For a single barrier, analytic expressions for $T(k)$ and $R(k)$ have been found to be[35,36]

$$R(k) = e^{-2ikl}\frac{(k^2-\hat{k}^2)\sin\hat{k}\Delta}{(k^2+\hat{k}^2)\sin\hat{k}\Delta - i2k\hat{k}\cos\hat{k}\Delta}, \tag{7}$$

and

$$T(k) = \frac{-2ik\hat{k}e^{ik\Delta}}{(k^2+\hat{k}^2)\sin\hat{k}\Delta - i2k\hat{k}\cos\hat{k}\Delta} \tag{8}$$

for $\hat{k}=\sqrt{k^2-U_0}$. It is straightforward to show that $|R|^2+|T|^2=1$, as required for conservation of energy.

For a high-impedance source and a duct that is uniform at the origin, so that $dS(x)/dx=0$ at $x=0$, the Euler equation states the volume velocity excitation, $u(0,t)$, to be

$$u(0,t) = -\frac{\sqrt{S(0)}}{\rho_0}\int_0^t \left.\frac{\partial\Psi(x,\tau)}{\partial x}\right|_{x=0} d\tau, \tag{9}$$

for ρ_0 the equilibrium density of air. (For a discussion of the effects of a bore that is sloped or curved at the input, see Ref. 38.) Setting $u(0,t)=e^{i\omega t}$ thus yields[35,36] the analytic Green's function for the impulse response radiated into the free field, as

$$G_f(x|0|\omega) = \frac{\rho_0 c}{\sqrt{S(0)}}\left(\frac{T(k)}{1-R(k)}\right)e^{-ik[x-(l+\Delta)]}. \tag{10}$$

The power spectrum is therefore

$$|G_f(x|0|\omega)|^2 = \frac{\rho_0^2c^2}{S(0)}g(k), \tag{11}$$

where

$$g(k) = \left|\frac{T(k)}{1-R(k)}\right|^2. \tag{12}$$

The time-independent pressure spectrum, $|P(k)|^2$, a measurable quantity at a point $x=L$ in the free field, is then

$$|P(k)|^2 = \beta g(k), \tag{13}$$

where β is a frequency-independent normalization constant,

$$\beta = \frac{\rho_0^2c^2}{S(0)S(L)}. \tag{14}$$

It may be noted that β is not directly measurable, since it depends on the area, $S(L)$, of the virtual infinite cone. For measurements near the duct mouth, however, it can be approximated as

$$\beta = \frac{\rho_0^2c^2}{S(0)S(l)}, \tag{15}$$

which is measurable. Since the foregoing analysis applies equally to sequences of potential functions (which may include, for example, an arbitrary baffle at the termination) for which $R(k)$ is the matricial reflection coefficient taken at the origin,[35,36] it is now possible to present an inverse solution for the noninvasive reconstruction of the potential and area functions of an unknown duct.

B. Inverse problem: Inverse potential scattering in duct acoustics

By adopting the simplifying assumption of one-dimensional propagation, it has been possible to derive an energy-conserving expression for the normalized, radiated spectrum that is a function of only the transmission and re-

flection coefficients of the duct potential function. Subsequently, since it is known in the quantum mechanical literature[40,41] that the potential function of a scattering system can be reconstructed from $R(k)$, but not from $T(k)$ alone, it becomes sensible to ask whether the unknown potential function can be reconstructed from the combined term, $T(k)/(1-R(k))$. More specifically, it may be asked whether $R(k)$ can be obtained from the radiated pressure, $g(k)$ (13). An answer in the affirmative would also allow quantities such as the input impedance to be derived, in situations where they cannot be measured.

In fact, it has been been proved by Aktosun,[42] in a quantum-mechanical context that generalizes completely to the acoustical setting, that $g(k)$ is equivalent to the real part of the quantity $[1+R(k)]/[1-R(k)]$. Letting $R(k)=a+ib$, the proof is straightforwardly derived since

$$\Re\left\{\frac{1+R(k)}{1-R(k)}\right\}=\Re\left\{\frac{[1+a+ib][1-(a-ib)]}{[1-(a+ib)][1-(a-ib)]}\right\} \tag{16}$$

so that

$$\Re\left\{\frac{1+R(k)}{1-R(k)}\right\}=\frac{\Re(1-|R|^2+2ib)}{|1-R(k)|^2}. \tag{17}$$

Since in an energy-conserving system such as the one presented here, it must be the case that $|T(k)|^2+|R(k)|^2=1$, it can be immediately seen that

$$\Re\left\{\frac{1+R(k)}{1-R(k)}\right\}=\frac{|T(k)|^2}{|1-R(k)|^2}, \tag{18}$$

cf. Eq. (12). Beginning from the quantum-mechanical Jost solution in terms of e^{ikx} for a wave propagating in the positive x direction, Aktosun has gone on to show that the imaginary part, $\lambda(k)$, of a complex quantity, $\Lambda(k)$, where

$$\Re[\Lambda(k)]=\Re\left\{\frac{1+R(k)}{1-R(k)}-1\right\}, \tag{19}$$

can be obtained by analytic continuation in the complex plane as

$$\lambda(k)=-\frac{1}{\pi}\mathrm{CPV}\int_{-\infty}^{\infty}\frac{\Re[\Lambda(s)]}{s-k}ds, \tag{20}$$

where CPV means that the integral must be evaluated as a Cauchy principal value. Setting $\Lambda(k)=\Re[\Lambda(k)]+i\lambda(k)$, substitution of Eq. (12) into Eq. (19) leads to the derivation of the reflectance, $R(k)$, from $g(k)$ as

$$R(k)=\frac{\Lambda(-k)}{2+\Lambda(-k)}. \tag{21}$$

[Note that, in contrast to the description given in, Ref. 42 the right-hand side of Eq. (21) depends on $-k$ rather than k. This is due to the acoustical convention that a wave propagating in the positive x direction be represented as e^{-ikx}.] For a duct that is uniform near the origin,[38] the input impedance is immediately identified as

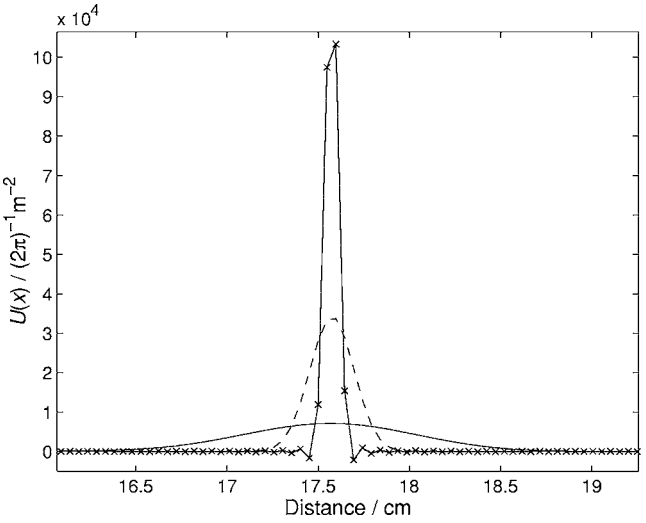

FIG. 4. Reconstruction of single barrier (see Fig. 3) from analytic data, at 180 (×), 20 (---) and 5 (—) kHz bandwiths, respectively.

$$Z_0=\frac{\rho c}{S(0)}\frac{1+R(k)}{1-R(k)}. \tag{22}$$

Transformation of $R(k)$ to the time domain then allows the potential function, $U(x)$, to be obtained by solution of the Marchenko integral equation.[40] Berryman and Greene[28] have proposed a fast matrix method for the numerical solution that also allows the area function to be recovered in terms of cylindrical segments if an initial value of $S(0)$ is supplied. Otherwise, the area function may be obtained[35,36] from Eq. (6), given initial values for $S(0)$ and $dS(x)/dx$ (although care must be taken with conditioning of the solution).

In this section, it has been shown that by conserving energy in a one-dimensional approximation to acoustic scattering, the wave-mechanical model of sound propagation allows the reflectance to be derived noninvasively from the radiated wave without any additional knowledge of the radiation impedance. We may now go on to examine the method through numerical simulations.

IV. NUMERICAL SIMULATIONS AND VALIDATION

First, the stability of the fast matrix method of Berryman and Greene[28] was affirmed. The method is preferred for computational solution of the Marchenko equation and inversion to the potential function from a temporal reflectance, $L(t)$. $R(k)$ was evaluated from the exact analytic expression of Eq. (7) at parameters appropriate to the barrier configuration of Fig. 3, for $l=17.5$ cm. Inverse Fourier transformation yielded $L(t)$. This initial step highlighted the problem of the "Gibbs phenomenon" in simulated data, since it is known that the Fourier transformation of band-limited data leads to numerical errors from windowing convolutions and ripple.[43] To avoid these numerical artifacts, $R(k)$ was first obtained at a high bandwidth of around 180 kHz and then low-pass filtered using a Gaussian filter over experimental ranges before transformation. The Berryman–Greene routines[28] were then coded in MATLAB. Figure 4 shows the resulting reconstruction of the single barrier from data simulated at high bandwidth, and data filtered at half-power points of 20 kHz (the

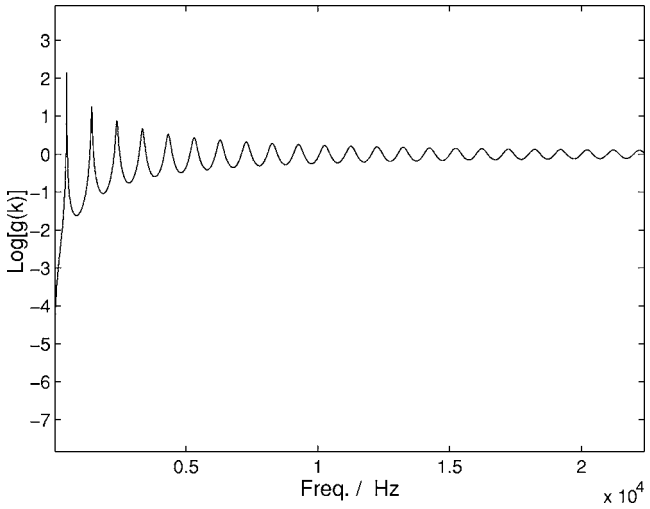

FIG. 5. Log$[g(k)]$ for configuration of Fig. 3 taken up to 20 kHz bandwidth.

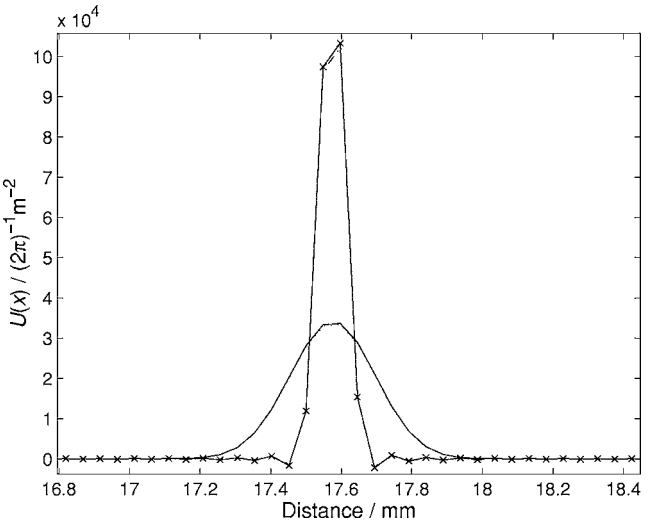

FIG. 7. Reconstruction of single barrier at 180 kHz bandwidth, from analytic data (×) and that obtained by Aktosun method (---). Reconstruction of single barrier at 20 kHz bandwidth, from analytic data (—) and that obtained by Aktosun method (···).

loudspeaker range) and 5 kHz (around experimental bandwidths and the plane-wave limit in speech acoustics). At high bandwidth, the square barrier is reconstructed to within 3% maximum error (up to a scaling factor of 2π) over three sample points, agreeing well with the spatial resolution of 0.48 mm predicted by Eq. (2). The effects of the Gibbs phenomenon manifest as a small amount of ripple around discontinuities. In contrast, for filtered data the spatial resolution falls to around 4 mm at a half-power point of 20 kHz and to 1.7 cm at 5 kHz, so that the Gibbs ringing is also smoothed. These results are in precise agreement with the predictions of Eq. (2) and it was concluded that numerical errors in the Berryman–Greene routines, and those due to transformation of simulated data, were effectively controlled.

Subsequently, the Aktosun integral equation (20) was solved by trapezium rule implemented in MATLAB, the two major numerical considerations being the avoidance of the poles at $s=k$ and the effect of truncating the limits of integration. The frequency-dependent part of the radiated power spectrum, $g(k)$, was obtained from Eq. (12) at a resolution of $\delta=10$ Hz and integrated up to $k \mp \delta$. A significantly narrower discretization will tend to lead to "divide by zero" errors around the poles and a wider discretization fails to resolve rapid variation in the spectrum. Equation (21) was then solved for varying limits in Eq. (20) to yield $R(k)$. At an effectively infinite bandwidth of 180 kHz, by which limits $g(k)=1$, it was found that the rms error in the derived reflectance [in comparison to the exact analytic solution (7)] was just 1.4×10^{-3}. Figure 5 shows that the oscillations in $g(k)$ are still evident at 20 kHz and thus, on truncation to these limits, the rms error rose slightly to 6.1×10^{-3}. Figure 6 demonstrates the nevertheless-close correspondence between the derived and analytic data. At 5 kHz truncation limits, the rms error increased to 7.5×10^{-3}, still only 0.8% of the maximum, however. Figure 7 shows that the potential-function reconstructions obtained from analytic and derived data agree to better than 1% maximum error, affirming the validity of the Aktosun proofs and numerical integration routines.

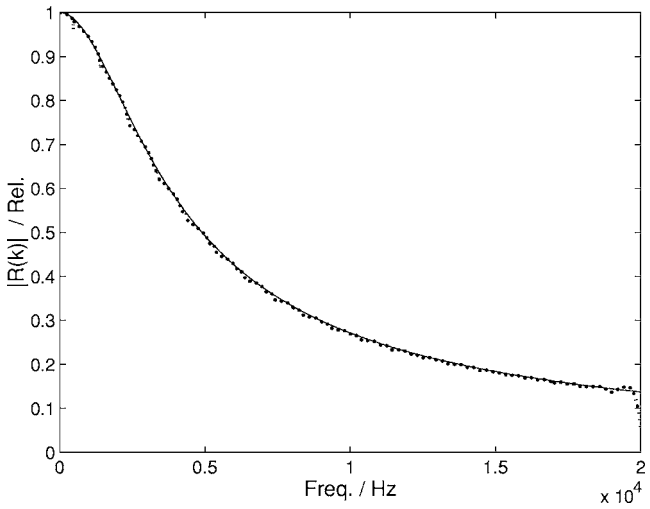

FIG. 6. $R(k)$: analytic (—) and derived by Aktosun method (···) at 20 kHz bandwidth.

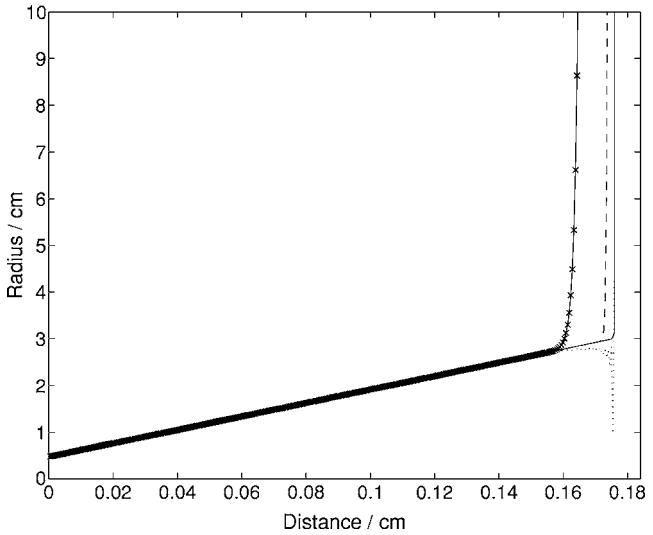

FIG. 8. Reconstruction of conical bore at 180 (···), 20 (---), and 5 (×) kHz bandwidths. Also shown: nominal radius (—).

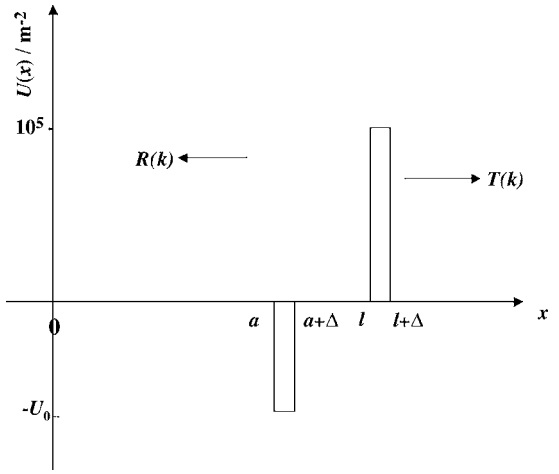

FIG. 9. Schematic potential-function profile of well-barrier pair, $U_0=6.0\times10^4$ m^{-2}, $\Delta=1$ mm, $a=17.1$ cm, $l=17.5$ cm.

(At experimental limits below 20 kHz, it was found that the integral can be performed more or less in real time on a 3.2 GHz PC with 2 Gbytes RAM.)

Figure 8 illustrates the area functions obtained from the reconstructed potential functions by solution of Eq. (6) for initial conditions $r_0=4.8$ mm, $r_l=3$ cm, and $dr(x)/dx|_{x=0}=(r_l-r_0)/l$. The expansion into the infinite conical baffle is narrowly resolved to around 0.5 mm at high bandwidth, with slight Gibbs ringing evident as before. The spatial resolution falls to around 4 mm and 1.7 cm at 20 and 5 kHz, respectively, again in full agreement with the predictions of Eq. (2).

Figure 9 illustrates a schematic well-barrier pair, a configuration generally corresponding to a negative curvature and duct constriction that will lower or raise a resonance depending on its position relative to the standing wave pattern.[37] Figure 10 illustrates the stability and narrow localization of this potential function reconstruction over space, affirming that cumulative errors found in other recursive layer-peeling algorithms[25] are well controlled in the Marchenko inversion. Figure 11 gives a magnified view; the errors and spatial resolutions at ideal and experimental bandwidths

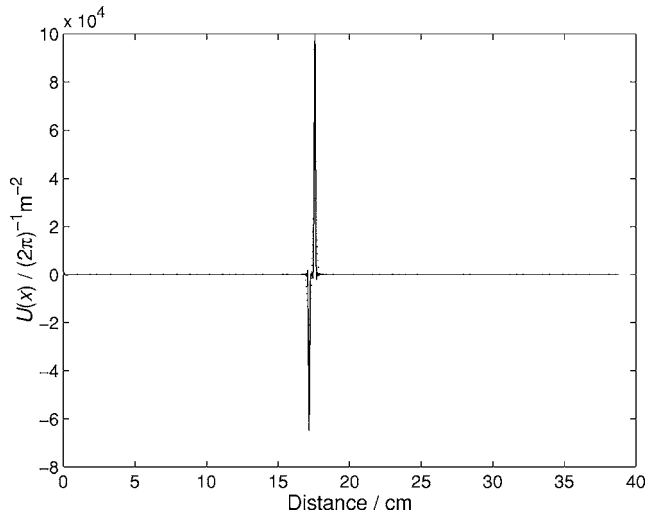

FIG. 10. Reconstruction of well-barrier corresponding to Fig. 9, from data derived by Aktosun method at 180 kHz bandwidth.

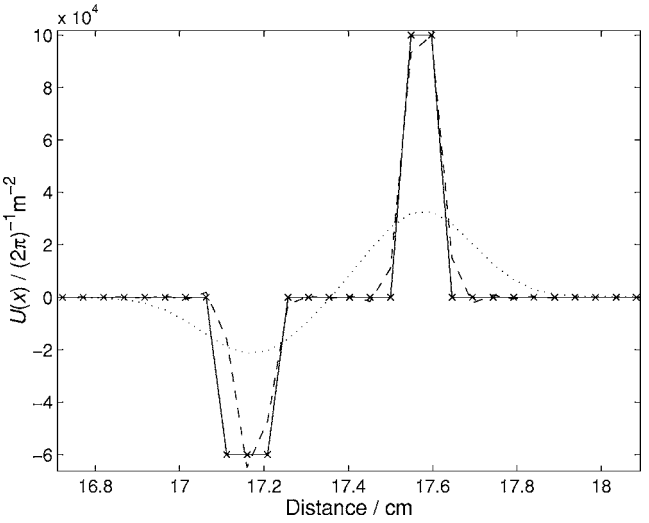

FIG. 11. Magnified view of Fig. 10. Nominal solution (×); data derived at 180 kHz (---) and 20 kHz (···) bandwidths.

are completely in line with previous results. On assumption of a cylindrical discretization of the duct and for a given value of $S(0)$, the Berryman–Greene also yields an area function in the equivalence set corresponding to any potential function. Figure 12 illustrates one such area function, reconstructed at various bandwidths and shown against the exact analytic solution defined by Eq. (6). As before, the resolution of the rapid changes in curvature is around 4 mm at 20 kHz bandwidth, falling to 1.7 cm at 5 kHz. It is clearly seen that the 4 mm resolution yields the bore profile rather accurately, in fact to better than 2.5% at the point of maximum constriction.

In this section, an analytic proof for deriving the wave-mechanical reflectance from the Jost solution has been validated in a one-dimensional approximation to duct acoustics. From the reflectance, the Marchenko equation for inversion to the potential function has been solved by the fast matrix method of Berryman and Greene and related area functions have also been obtained. The "wave mechanical" method has

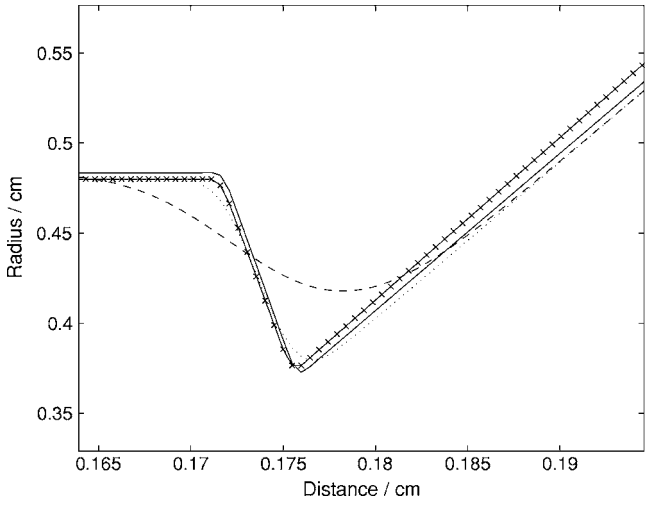

FIG. 12. Reconstruction of radius function corresponding to Figs. 9 and 11. Nominal solution (×), and from data derived at 180 (—), 20 (···), and 5 (---) kHz bandwidths.

been tested on both barriers and wells and so generalizes completely to compound potential functions that characterize highly localized constrictions and expansions,[37] which may correspond to leaks and blockages in a pipe.

V. DISCUSSION

Although the wave-mechanical method for the noninvasive measurement of the shape of an acoustical duct has been validated in principle, the experimental implementation will require consideration of several, familiar, details. First, the method assumes a high-impedance, flat spectrum, source. Recent work has described[44] such a source in terms of the maximum length sequence excitation of a piezoelectric driver mounted in a rigid plate, for example. Alternatively the "sine-wave packet" technique, already in use for APR measurements,[13] could be tried. Nevertheless, deconvolution of the input pulse from the measured data, a well-known problem,[1] will be necessary, requiring initial measurements with a nonreflecting tube.

Second, the scale factor β (14) must be calibrated and normalized. As discussed, it may be estimated from Eq. (15) for measurements near the mouth. Subsequently, a short lead-in tube of known dimensions could be reconstructed by iterative adjustment of β to an acceptable level of accuracy. Indeed, a similar procedure is currently standard practice in the control of pressure offsets.[15]

Third, the Marchenko equation does not allow for propagation losses and so the Berryman–Greene method is unlikely to be suitable for the reconstruction of long or very narrow objects in which boundary layer viscous and thermal effects, described by a complex wave number,[27] become significant. However, it is a great advantage of the Aktosun method that it does, in fact, generalize to a wave number in the upper half of the complex plane. Further work can, therefore, examine the derivation of the lossy reflectance, which would allow the application of standard lossy layer peeling algorithms.

Finally, the method is especially promising for application to the "classic" low-frequency problem of the inversion to the vocal tract shape from the speech signal,[45] although further consideration must be given to the deconvolution of the glottal wave form[46,47] and to calibration of the scale factor.

VI. CONCLUSIONS

The proposed wave-mechanical method for reconstruction of the potential and area functions of an unknown object from the radiated wave demonstrates highly satisfactory numerical stability and accuracy on simulated data, and is a promising technique for noninvasive acoustical measurements. In particular, it indicates how the long lengths of control tubing necessary for direct measurement of the reflectance can be eliminated, substantially reducing propagation losses at high frequency. Although the technique promises up to a fourfold improvement in spatial resolution, improvements will be limited in practice as the one-dimensional approximation to the radiation impedance becomes less appropriate over the increased frequency range. A more detailed examination of the trade off between improved losses and limits of the one-dimensional model remains to be undertaken. Nevertheless, the results presented here are likely be immediately relevant to many narrow bore applications, and to be particularly interesting for the speech inverse problem.

ACKNOWLEDGMENTS

The authors gratefully acknowledge the support in the UK of EPSRC Grant No. GR/S72177/01. They also thank Jonathan Kemp for many valuable discussions on higher-mode theory and Brendan Aengenheister in the Open University workshop for the construction of test cones.

[1] B. J. Forbes, D. B. Sharp, J. A. Kemp, and A. Li, "Singular system methods in acoustic pulse reflectometry," Acta. Acust. Acust. **89**, 743–753 (2003).
[2] J. Schroeter and M. M. Sondhi, "Techniques for estimating vocal-tract shapes from the speech signal," IEEE Trans. Speech Audio Process. **2**, 133–150 (1994).
[3] M. R. Schroeder, "Determination of the geometry of the human vocal tract by acoustic measurements," J. Acoust. Soc. Am. **41**, 1002–1010 (1967).
[4] P. Mermelstein, "Determination of the vocal tract shape from measured formant frequencies," J. Acoust. Soc. Am. **41**, 1283–1294 (1967).
[5] M. M. Sondhi and B. Gopinath, "Determination of vocal tract shape from impulse response at lips," J. Acoust. Soc. Am. **49**, 1867–1873 (1971).
[6] M. M. Sondhi and J. R. Resnick, "The inverse problem for the vocal tract: Numerical methods, acoustical experiments and speech synthesis," J. Acoust. Soc. Am. **73**, 985–1002 (1983).
[7] I. Marshall, "Acoustic reflectometry with an arbitrarily short source tube," J. Acoust. Soc. Am. **91**, 3558–3564 (1992).
[8] I. Marshall, "Impedance reconstruction methods for pulse reflectometry," Acustica **76**, 118–128 (1992).
[9] D. B. Sharp, "Increasing the length of tubular objects that can be measured using acoustic pulse reflectometry," Meas. Sci. Technol. **9**, 1469–1479 (1997).
[10] D. B. Sharp and D. M. Campbell, "Leak detection in pipes using acoustic pulse reflectometry," Acust. Acta Acust. **83**, 560–566 (1997).
[11] J. A. Kemp, J. M. Buick, and D. M. Campbell, "Practical improvements to acoustic pulse reflectometry," Proceedings of the International Symposium on Musical Acoustics Perugia, Italy 2001, No. 2, pp. 391–394.
[12] J. M. Buick, J. A. Kemp, D. B. Sharp *et al.*, "Distinguishing between similar tubular objects using pulse reflectometry: A study of trumpet and cornet leadpipes," Meas. Sci. Technol. **13**, 750–757 (2002).
[13] A. Li, D. B. Sharp, and B. J. Forbes, "Improving the high frequency content of the input signal in acoustic pulse reflectometry," Proceedings of the International Symposium on Musical Acoustics, Perugia, Italy, 2001, pp. 391–394.
[14] B. J. Forbes, J. A. Kemp, and D. B. Sharp, "Pulse reflectometry as an acoustical inverse problem: Regularisation of the bore reconstruction," Proceedings of the First Pan-American/Iberian Meeting on Acoustics incorporating the 144th Meeting of the A.S.A, Cancun, Mexico, 2002.
[15] A. Li, D. B. Sharp, B. J. Forbes, and J. A. Kemp, "The problem of DC offset in the measurement of impulse response using acoustic pulse reflectometry," Proceedings of the Institute of Acoustics, Salford, UK, 2002, Vol. 24, No. 2.
[16] A. Li and D. B. Sharp, "Reducing the source tube to improve the bandwidth of acoustic pulse reflectometry," Proceedings of the Stockholm Music Acoustics Conference (SMAC), Stockholm, Sweden, 2003.
[17] P. Ladefoged, R. Harshman, L. Goldstein, and L. Rice, "Generating vocal tract shapes from formant frequencies," J. Acoust. Soc. Am. **64**, 1027–1035 (1978).
[18] L.-J. Boë, P. Perrier, and G. Bailly, "The geometric vocal tract variables controlled for vowel production: Proposals for constraining acoustic-to-articulatory inversion," J. Phonetics **20**, 27–38 (1992).
[19] J. Schoentgen and S. Ciocea, "Kinematic formant-to-area mapping," Speech Commun. **21**, 227–244 (1997).
[20] P. Badin, D. Beautemps, R. Laboissière *et al.*, "Recovery of vocal-tract geometry from formants for vowels and fricative consonants using a midsaggital-to-area function conversion model," J. Phonetics **23**, 221–229 (1995).

[21]D. Beautemps, P. Badin, and R. Laboissière, "Deriving vocal-tract area functions from midsaggital profiles and formant frequencies: A new model for vowels and fricative consonants based on experimental data," Speech Commun. **16**, 27–47 (1995).
[22]J. Claerbout, *Fundamentals of Geophysical Data Processing* (McGraw-Hill, New York, 1976.
[23]Rakesh, "Impedance inversion from transmission data for the wave equation," Wave Motion **24**, 263–274 (1996).
[24]Rakesh and P. Sacks, "Characterisation of transmission data for Webster's horn equation," Inverse Probl. **16**, L9–L24 (2000).
[25]N. Amir, G. Rosenhouse, and U. Shimony, "A discrete model for tubular acoustic systems with varying cross-section—The direct and inverse problems. I II. Theory and experiment," Acustica **81**, 450–474 (1995).
[26]J. Agulló and S. Cardona, "Time-domain deconvolution to measure reflection functions for discontinuities in waveguides," J. Acoust. Soc. Am. **97**, 1950–1957 (1995).
[27]D. H. Keefe, "Acoustical wave propagation in cylindrical ducts: Transmission line parameter approximations for isothermal and nonisothermal boundary conditions," J. Acoust. Soc. Am. **75**, 58–62 (1984).
[28]J. G. Berryman and R. R. Greene, "Discrete inverse methods for elastic waves in layered media," Geophysics **45**, 213–233 (1980).
[29]V. Pagneux, N. Amir, and J. Kergomard, "A study of wave propagation in varying cross-section waveguides by modal decomposition. I. Theory and validation," J. Acoust. Soc. Am. **100**, 2034–2048 (1996).
[30]C. Hazard and V. Pagneux, "Improved multimodal approach in waveguides with varying cross-section," Proceedings of the 17th International Congress on Acoustics, Rome, 2001, Vol. 25, No. 1–3, pp. 3, 4.
[31]J. A. Kemp, "Multimodal propagation in acoustic horns," Proceedings of the International Symposium on Musical Acoustics, Perugia, Italy, 2001, Vol. 2, pp. 521–524.
[32]J. A. Kemp, "Theoretical and experimental study of wave propagation in brass musical instruments," Ph.D. thesis, University of Edinburgh, 2002.
[33]A. M. Bruneau, M. Bruneau, P. H. Herzog, and J. Kergomard, "Boundary layer attenuation of higher order modes in waveguides," J. Sound Vib. **119**, 15–27 (1987).
[34]A. H. Benade and E. V. Jansson, "On plane and spherical waves with nonuniform flare. I. Theory of radiation, resonance frequencies and mode conversion," Acustica **31**, 79–98 (1974).
[35]B. J. Forbes, "A potential-function analysis of speech acoustics," Ph.D. thesis, Department of Physics, King's College London, Strand, London WC2R 2LS, 2000.
[36]B. J. Forbes, E. R. Pike, and D. B. Sharp, "The acoustical Klein-Gordon equation: The wave-mechanical step and barrier functions," J. Acoust. Soc. Am. **114**, 1291–1302 (2003).
[37]B. J. Forbes and E. R. Pike, "The acoustical Klein-Gordon equation: A time-independent perturbation analysis," Phys. Rev. Lett. **93**, 1–4 (2004).
[38]B. J. Forbes, "The acoustical impedance defined by 'wave function' solutions of the reduced Webster equation," Phys. Rev. E **72**(1), 1–4 (2005).
[39]S. Gasiorowicz, *Quantum Physics* (Wiley, New York, 1974) pp. 469–471.
[40]K. Chadan and P. C. Sabatier, *Inverse Problems in Quantum Scattering Theory*, 2nd ed., (Springer, New York, 1989), Chap. XVII.
[41]Rakesh, "Potential inversion from transmission data for the one-dimensional wave equation," Wave Motion **25**, 319–329 (1997).
[42]T. Aktosun, "Construction of the half line potential from the Jost function," Inverse Probl. **20**, 859–876 (2004).
[43]N. Amir, U. Shimony, and G. Rosenhouse, "Losses in tubular acoustic systems—Theory and experiment in the sampled time and frequency domains," Acust. Acta Acust. **82**, 1–8 (1996).
[44]M. H. F. de Salis, N. V. Movchan, and D. J. Oldham, "Characterising holes in duct walls using resonance frequencies," J. Acoust. Soc. Am. **111**, 2583–2593 (2002).
[45]T. Aktosun, "Inverse scattering for vowel articulation with frequency-domain data," Inverse Probl. **21**, 899–914 (2005).
[46]A. Kounoudes, P. A. Naylor, and M. Brookes, "The DYPSA algorithm for estimation of glottal closure instants in voiced speech," Proc. ICASSP, 2002.
[47]J. Epps, J. R. Smith, and J. Wolfe, "A novel instrument to measure acoustic resonances of the vocal tract during phonation," Meas. Sci. Technol. **8**, 1112–1121 (1997).